Journal of Magnetic Resonance **143,** 387–390 (2000)
doi:10.1006/jmre.1999.1998, available online at http://www.idealibrary.com on IDEAL®

COMMUNICATIONS

New Techniques for the Measurement of C′N and C′H^N *J* Coupling Constants across Hydrogen Bonds in Proteins

Axel Meissner and Ole Winneche Sørensen

Department of Chemistry, Carlsberg Laboratory, Gamle Carlsberg Vej 10, DK-2500 Valby, Denmark

Received September 22, 1999; revised December 1, 1999

Two new two- or three-dimensional NMR methods for measuring $^{3h}J_{C'N}$ and $^{2h}J_{C'H}$ coupling constants across hydrogen bonds in proteins are presented. They are tailored to suit the size of the TROSY effect, i.e., the degree of interference between dipolar and chemical shift anisotropy relaxation mechanisms. The methods edit 2D or 3D spectra into two separate subspectra corresponding to the two possible spin states of the $^1H^N$ spin during evolution of ^{13}CO coherences. This allows $^{2h}J_{C'H}$ to be measured in an E.COSY-type way while $^{3h}J_{C'N}$ can be measured in the so-called quantitative way provided a reference spectrum is also recorded. A demonstration of the new methods is shown for the ^{15}N,^{13}C-labeled protein chymotrypsin inhibitor 2.

Key Words: ^hJ; **hydrogen bonds; TROSY; E.COSY; S^3 editing.**

The discovery of *J* couplings across hydrogen bonds in biomolecules (*1*) has added new very important constraints in structure determinations of biological macromolecules that so far could only be inferred indirectly. The largest *J* coupling constants across hydrogen bonds are observed in RNA (*1*) and DNA (*2*, *3*) but also $^{3h}J_{C'N}$ in proteins has proven to be of sufficient magnitude for detection (*4–7*) and there is also a report on measurement of $^{2h}J_{C'H}$ (*8*).

Because techniques for measurement of *J* coupling constants across hydrogen bonds necessarily require such a coupling for coherence transfer, their small magnitudes make the techniques inherently of low sensitivity. Hence it is important to optimize the techniques in any possible way as increasing linewidths for larger biomolecules reduce the sensitivity further. In this Communication we present two techniques for the measurement of $^{3h}J_{C'N}$ and $^{2h}J_{C'H}$ that are designed to suit two different ranges of the TROSY (*9*) effect. In this respect, they are similar to earlier work for measurement of one-bond *J* and residual dipolar ^1H–^{15}N coupling constants in orienting media where techniques were suggested for three different ranges of the TROSY effect. This study extends work on ^hJ coupling constants by Pervushin *et al.* (*2*) and Grzesiek and Bax and colleagues (*4–7*).

In the range of small TROSY effects, the two doublet resonances of ^1H or ^{15}N spectra in amide groups are of similar intensity and both doublet components are useful for measurement of ^hJ coupling constants. In contrast, for large TROSY effects it is only the TROSY peak that exhibits sufficient sensitivity for detection and the pulse sequences must take this into account.

There are two different schools of thought when it comes to measurement of coupling constants, which also apply for measurement of those across hydrogen bonds. E.COSY-type methods (*10–12*) typically combined with spin-state-selective (S^3) editing (*13–15*) work on the basis of direct measurement of peak displacements in different sections of multidimensional spectra. On the other hand, so-called quantitative methods (*16*) extract coupling constants from intensity ratios of different peaks. In this Communication we concentrate on measurement of $^{2h}J_{C'H}$ by S^3-edited E.COSY methods but, in full analogy to earlier work, $^{3h}J_{C'N}$ can be measured from the same data by the quantitative approach provided that a reference spectrum with a different evolution time for $^{3h}J_{C'N}$ is recorded (*4–7*). Our experiments allow measurement of arbitrarily small $^{2h}J_{C'H}$ including their signs if the associated $^{3h}J_{C'N}$ is large enough to generate cross peaks of adequate intensity. This is in contrast to the method proposed in Ref. (*8*) that also exhibits less favorable transverse relaxation characteristics because of long delays with transverse H^N magnetization. The method proposed in Ref. (*2*) includes detection of anti-TROSY peaks, which is unfavorable for large molecules where it leads to significantly reduced sensitivity for one of the two subspectra used for S^3 E.COSY-type measurement of a passive ^hJ coupling constant. Our methods proposed below do not detect anti-TROSY peaks.

Figure 1a shows the pulse sequence applicable for small TROSY effects. It is conceptually similar to the one proposed by Pervushin *et al.* (*2*) for the measurement of *J* couplings across hydrogen bonds in DNA and the editing into two subspectra by the final TROSY-type element is identical to what was used for one-bond ^1H–^{15}N coupling constants in isotropic and bicelle solutions in Ref. (*17*). In the t_1 period with ^{13}CO evolution the two coherences corresponding to specific spin

1090-7807/00 $35.00

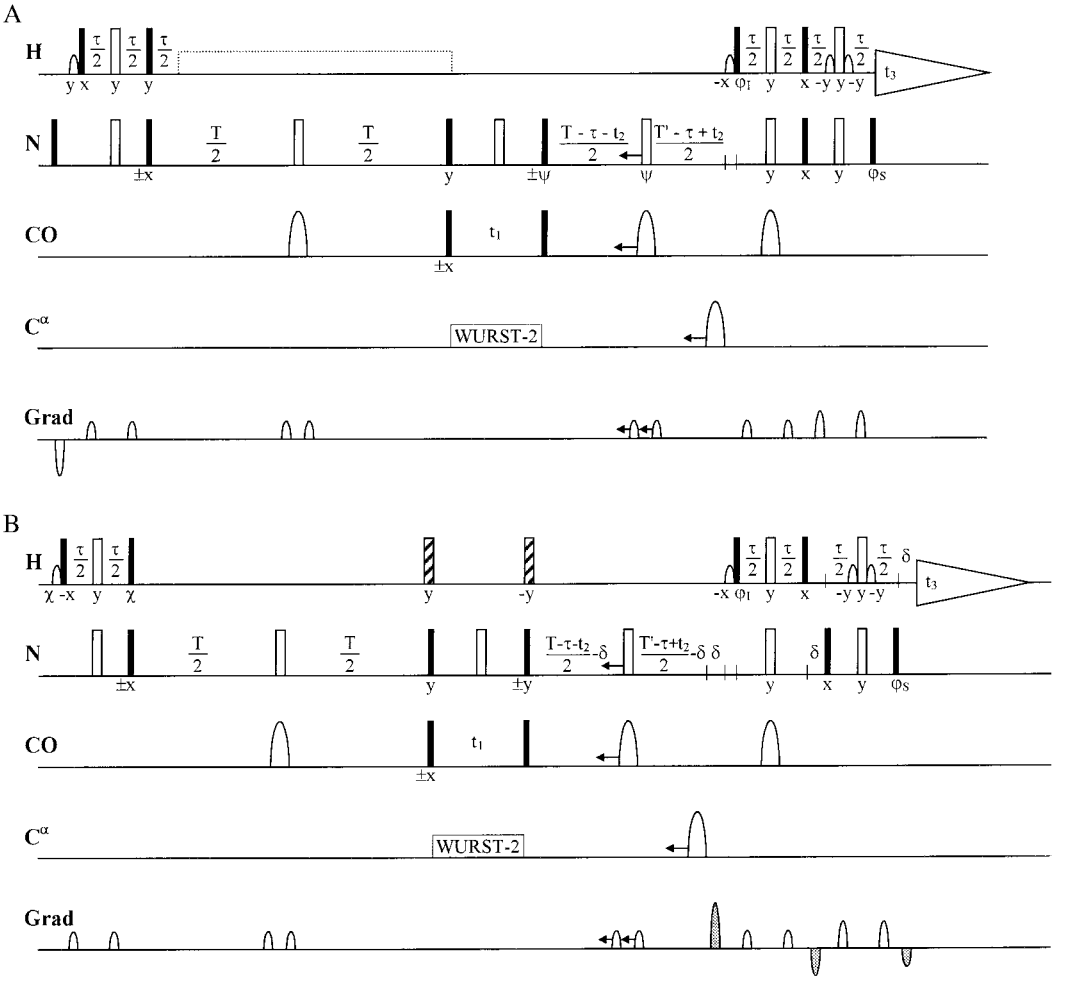

FIG. 1. 3D S^3 HNCO pulse sequences for the measurement of $^{2h}J(H^N, CO)$ coupling constants across hydrogen bonds in proteins. Filled and open bars represent $\pi/2$ and π pulses, respectively. Selective $\pi/2$ water pulses and selective π carbon pulses are shown as open bell shapes. $\tau = (2J_{N,H})^{-1}$; $T = n(^1J_{N,CO})^{-1}$, $n = 1, 2$; $T' = T - 2$ (duration of selective water $\pi/2$ pulse); δ = gradient delay. The pulse phases are indicated below the pulses. Pulse phases with the prefix $\pm$ indicate independent two-step phase cycles with alternating receiver phase. (a) S^3 HNCO for molecules with small TROSY effects. Phase settings for recording semi-TROSY peaks in t_2/t_3. The phase ψ is cycled to create two data sets that contain both semi-TROSY resonances of the multiplets for the echo and antiecho pathways, respectively: $A(\psi = x$; receiver $= x)$ is recorded with $(\varphi_I = y$; $\varphi_S = -y)$ and with $(\varphi_I = -y$; $\varphi_S = y)$, and the same for $B(\psi = y$; receiver $= y)$. Then $(A - B)(\varphi_I = y$; $\varphi_S = -y)$ and $(A + B)(\varphi_I = -y$; $\varphi_S = y)$ are echo and antiecho, respectively, for the subspectrum containing the lower left multiplet components while $(A - B)(\varphi_I = -y$; $\varphi_S = y)$ and $(A + B)(\varphi_I = y$; $\varphi_S = -y)$ are echo and antiecho, respectively, for the subspectrum containing the upper right multiplet components. The positions of the multiplet components are interchanged on our Bruker DRX 600 instrument. States-TPPI is applied on the $\pi/2$ pulse before t_1. (b) S^3 HNCO TROSY for molecules with larger TROSY effects. In order to include the native S spin magnetization in the TROSY resonance, the phase χ must be $-y$ on our Varian Unity Inova spectrometers while it must be y on our Bruker DRX 600 instrument. States-TPPI is applied on the $\pi/2$ pulse before t_1. In t_2 echo and antiecho data sets are generated in combination with the shaded pulsed field gradients. The phase settings for echo and antiecho on the Varian instruments are $\{\varphi_I = y$; $\varphi_S = y\}$ and $\{\varphi_I = -y$; $\varphi_S = -y\}$, respectively, while it would be reversed on the Bruker instrument. Two data sets are recorded without (A) and with (B) two composite π pulses indicated as hatched open bars on the proton channel; they constitute the two edited subspectra. 2D pulse sequences are obtained by setting $t_2 = 0$ and omitting the C^α pulse. The $3^hJ(N, CO)$ coupling constants can be measured simultaneously with $^{2h}J(H^N, CO)$ using the quantitative approach as described elsewhere (*4–7*).

states of the H^N proton are subsequently both transferred to ^{15}N coherences while maintaining the same H^N spin states. Then the double S^3CT (or TROSY) (*18*) element separates the two components into the subspectra corresponding to the two different spin states of the attached ^{15}N spins in the t_3 period and thereby also the different ^1H spin states in the t_1 and t_2 dimensions. These two subspectra are constructed from the same data sets (see Fig. 1 legend). As in Ref. (*17*), it is advantageous to select the semi-TROSY peaks in $\{t_2, t_3\}$ rather than the pair of TROSY and anti-TROSY peaks (*2*). However, the fact that this pulse sequence involves anti-TROSY resonances in at least one of the dimensions makes it unsuitable for molecules exhibiting large TROSY effects.

Figure 1b shows the pulse sequence that is recommended for molecules with large TROSY effects where only the TROSY resonances are exploited. Hence heteronuclear gradient echoes

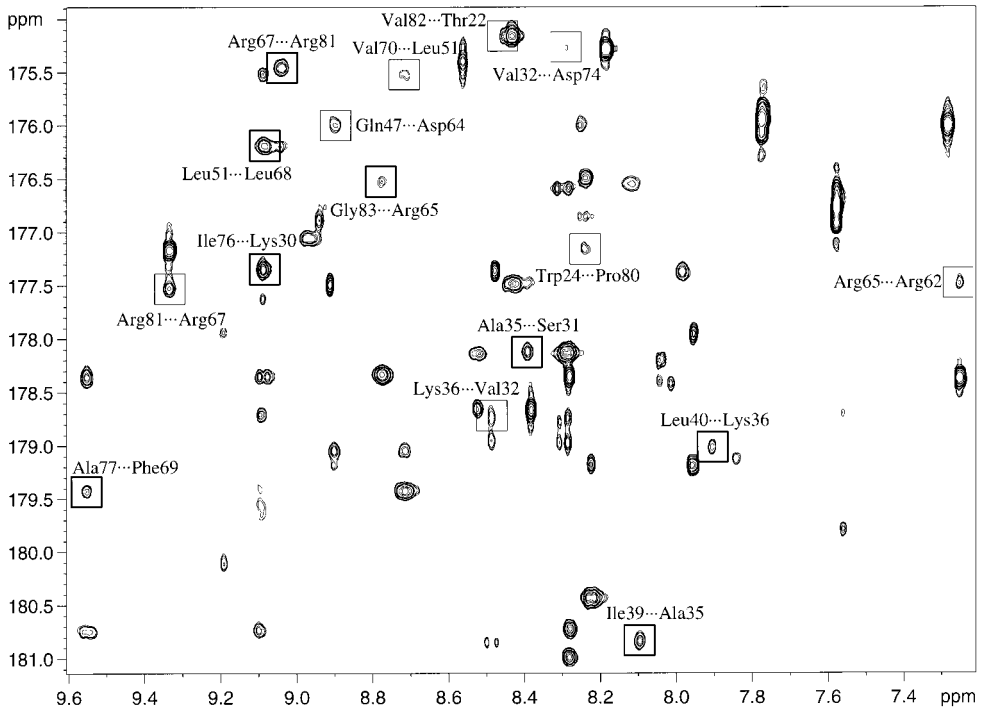

FIG. 2. Excerpt from the 2D S^3 HNCO TROSY experiment of $^{15}N,^{13}C$-labeled CI2 19–83 (90% H_2O/10% D_2O, 25°C, pH 4.2, 9 mg in 300 μl) recorded with the pulse sequence in Fig. 1b (^1H–^{15}N echo and subspectrum without the hatched π^H pulses) on a Varian Unity Inova 800 MHz spectrometer. Parameters: relaxation delay 1.5 s, T = 133.3 ms; τ = 5.43 ms; t_1(max) = 48.0 ms; 512 scans for each t_1 increment. Sinc-shaped (*21*) selective $\pi/2$ water pulses (1000.0 μs) and iBurp (*22*) selective carbon π pulses (930.0 μs) were used. Rectangular $\pi/2$ carbonyl pulses were calibrated to have a zero excitation profile in the C^α region. Adiabatic decoupling of C^α covering 20 ppm was applied using WURST-2 (*23*). The relative gradient strengths of the shaded gradients are −4.375:1.875:1.250 for echo selection. The other gradients are arranged in self-compensating pairs with relative amplitudes of 0.8 in the initial INEPT transfer, 1.0 in the T periods, 1.0 in the first S^3CT element of TROSY transfer, and 6.0 in the final S^3CT/watergate element. Data matrices of 192 × 2048 points covering 2000 × 12000 Hz were zero-filled to 2048 × 4096 prior to Fourier transformation and the window function was cosine in both dimensions. Boxes in the spectrum indicates cross peaks from H^N–CO correlations across hydrogen bonds. Representative sections for the cross peaks in the bold boxes are shown in Fig. 3.

can be employed in contrast to the sequence in Fig. 1a, which improves artifact and solvent suppression. The two subspectra corresponding to the different ^1H spin states in the ^{13}CO dimension are recorded separately, with and without the two hatched ^1H π pulses, respectively. The inherent reduction in effective sensitivity by $\sqrt{2}$, everything else equal, is compensated by inclusion of the native ^{15}N magnetization.

An experimental demonstration of the described methods is shown in Fig. 2 with an excerpt from a ^{15}N–^1H 2D S^3 HNCO TROSY spectrum of $^{15}N,^{13}C$-labeled chymotrypsin inhibitor 2 19–83 (CI2) recorded with the pulse sequence in Fig. 1b. Several cross peaks representing J couplings across hydrogen bonds are observed and a few examples of measurement of these $^{2h}J_{C'H}$ from sections from the two subspectra are shown in Fig. 3. CI2 was expressed, purified, and $^{15}N,^{13}C$-labeled as described previously (*19*, *20*).

A total of 16 hydrogen bonds could be identified in CI2 from the spectra recorded (all framed in Fig. 2) while 3 of the $^{2h}J_{C'H}$ coupling constants could not be measured in the 2D spectra due to spectral overlap. The coupling constants range up to about 1 Hz and both signs occur although most of them are positive. As also mentioned by other authors the major limitation for determining accurate values of the coupling constants across hydrogen bonds is the inherent low sensitivity of the experiments. One interesting aspect of our pulse sequences in Fig. 1 in comparison to the approach in Ref. (*8*) is that a hydrogen bond, Val32–Asp74, could be identified although the corresponding $^{2h}J_{C'H}$ is zero.

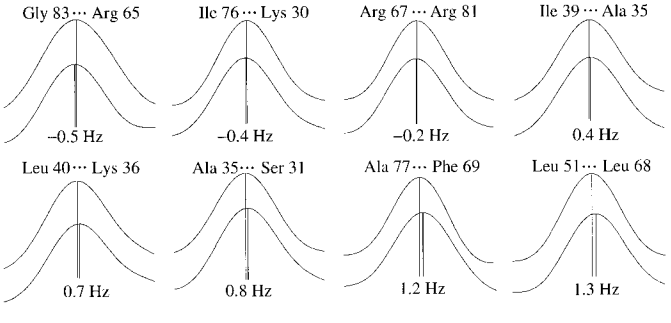

FIG. 3. 1D sections from the cross peaks marked with bold boxes in Fig. 2. The shift between the multiplet components of subspectrum A (top sections) and subspectrum B (bottom sections) is given below the traces and represents the $^{2h}J(H^N, CO)$ coupling constants. The sign is given relative to $^3J_{(H^N,CO)}$ of the protein backbone which is assumed to be positive.

Even for the relatively small protein CI2 (65 amino acids) exhibiting only a modest TROSY effect at 800 MHz it was found that the sensitivity of the approach in Fig. 1a was inadequate in the subspectrum involving the anti-TROSY ^{15}N resonance during the long T delays. An option for improvement is to direct the native ^{15}N magnetization to the ^{15}N anti-TROSY resonance in the first T delay and further combine it with an ^{1}H π pulse simultaneous with the first ^{13}CO $\pi/2$ pulse. Nevertheless, the approach in Fig. 1b remains the one of choice for CI2 at 800 MHz as these options only even out the peak intensities in the two subspectra. For very small TROSY effects decoupling of protons in the first T delay is an option that slows down relaxation.

In conclusion, we have described two new methods for the measurement of J couplings across hydrogen bonds in proteins suited to different ranges of the TROSY effect. They combine quantitative and E.COSY approaches so that $^{3h}J_{C'N}$ and $^{2h}J_{C'H}$ coupling constants can be measured from the same data sets.

ACKNOWLEDGMENTS

The spectra presented have been recorded on the Varian Unity Inova 800 MHz spectrometer of the Danish Instrument Center for NMR Spectroscopy of Biological Macromolecules at Carlsberg Laboratory. We thank Flemming M. Poulsen and Mathilde H. Lerche for the ^{15}N,^{13}C-labeled CI2 sample.

REFERENCES

1. A. J. Dingley and S. Grzesiek, *J. Am. Chem. Soc.* **120,** 8293–8297 (1998).
2. K. Pervushin, A. Ono, C. Fernandez, T. Szyperski, M. Kainosho, and K. Wüthrich, *Proc. Natl. Acad. Sci. USA* **95,** 14147–14151 (1998).
3. A. J. Dingley, J. E. Masse, R. D. Peterson, M. Barfield, J. Feigon, and S. Grzesiek, *J. Am. Chem. Soc.* **121,** 6019–6027 (1999).
4. F. Cordier and S. Grzesiek, *J. Am. Chem. Soc.* **121,** 1601–1602 (1999).
5. G. Cornilescu, J.-S. Hu, and A. Bax, *J. Am. Chem. Soc.* **121,** 2949–2950 (1999).
6. G. Cornilescu, B. E. Ramirez, M. K. Frank, G. M. Clore, A. M. Gronenborn, and A. Bax, *J. Am. Chem. Soc.* **121,** 6275–6279 (1999).
7. Y.-X. Wang, J. Jacob, F. Cordier, P. Wingfield, S. J. Stahl, S. Lee-Huang, D. Torchia, S. Grzesiek, and A. Bax, *J. Biomol. NMR* **14,** 181–184 (1999).
8. F. Cordier, M. Rogowski, S. Grzesiek, and A. Bax, *J. Magn. Reson.* **140,** 510–512 (1999).
9. K. Pervushin, R. Riek, G. Wider, and K. Wüthrich, *Proc. Natl. Acad. Sci. USA* **94,** 12366–12371 (1997).
10. C. Griesinger, O. W. Sørensen, and R. R. Ernst, *J. Am. Chem. Soc.* **107,** 6394–6395 (1985).
11. C. Griesinger, O. W. Sørensen, and R. R. Ernst, *J. Chem. Phys.* **85,** 6837–6852 (1986).
12. C. Griesinger, O. W. Sørensen, and R. R. Ernst, *J. Magn. Reson.* **75,** 474–492 (1987).
13. A. Meissner, J. Ø. Duus, and O. W. Sørensen, *J. Magn. Reson.* **128,** 92–97 (1997).
14. A. Meissner, J. Ø. Duus, and O. W. Sørensen, *J. Biomol. NMR* **10,** 89–94 (1997).
15. M. D. Sørensen, A. Meissner, and O. W. Sørensen, *J. Biomol. NMR* **10,** 181–186 (1997).
16. A. Bax, D. Max, and D. Zax, *J. Am. Chem. Soc.* **114,** 6923–6925 (1992).
17. M. Lerche, A. Meissner, F. M. Poulsen, and O. W. Sørensen, *J. Magn. Reson.* **140,** 259–263 (1999).
18. A. Meissner, T. Schulte-Herbrüggen, J. Briand, and O. W. Sørensen, *Mol. Phys.* **95,** 1137–1142 (1998).
19. P. Osmark, P. Sørensen, and F. M. Poulsen, *Biochemistry* **32,** 11007–11014 (1993).
20. J. C. Madsen, O. W. Sørensen, P. Sørensen, and F. M. Poulsen, *J. Biomol. NMR* **3,** 239–244 (1993).
21. A. J. Temps and C. F. Brewer, *J. Magn. Reson.* **56,** 355–372 (1984).
22. H. Geen and R. Freeman, *J. Magn. Reson.* **93,** 93–141 (1991).
23. Ē. Kupče and G. Wagner, *J. Magn. Reson. B* **109,** 329–333 (1995).